

Chapter 14

Real-Time Interactive MRI for Guiding Cardiovascular Surgical Interventions

Michael Guttman, Keith Horvath, Robert Lederman,
and Elliot McVeigh

Abstract

Real-time magnetic resonance imaging (rtMRI) is a compelling modality for guidance of surgical interventions. An effective toolkit for planning and guidance of surgery using rtMRI includes continuously updated images with excellent soft tissue contrast, devices that are visible in the images, interactively adjustable imaging parameters, simultaneous imaging and display of multiple intersecting oblique planes, and the ability to measure blood flow and perfusion. MRI has the benefit of not exposing the patient, physician, or staff to ionizing radiation from X-rays. This chapter describes the initial experience in the development of minimally invasive surgical implantation of an aortic valve in the beating heart, using continuously updated rtMRI. The potential benefits of this approach include reduction of patient trauma from open heart surgery using cardiopulmonary bypass, and the ability to implant a more robust device than can be delivered by catheter-based methods. Since the heart is a moving target, the surgeon is guided by continuously updated images, rather than those previously acquired as in stereotactic procedures.

14.1 Introduction

Minimally invasive approaches to cardiac surgical therapies are under active investigation to reduce trauma and recovery time [Doty et al. 2000; Vassiliades et al. 2005; Lutter et al. 2004]. Therapies traditionally requiring open-chest access are now being carried out through small incisions. Without direct access to the target, approaches under development deploy robotic tools under the surgeon's control to administer therapy with fiber optics, providing visual guidance. However, these approaches still require emptying the heart of blood to allow unobstructed visualization, and the heart is arrested to operate on a stationary target.

Real-time magnetic resonance imaging (rtMRI) provides views of anatomy and invasive devices in a beating heart with circulating blood.

Excellent anatomical detail is available due to inherent soft tissue contrast and oblique thin-slice imaging. Complementary functional information such as flow, ventricular ejection fraction, and perfusion are readily obtained. The effect of interventional therapies such as radiofrequency ablation, cryoablation, and direct injections can be observed quickly in rtMRI.

Advantages of MR arise not only from the superior soft tissue contrast, but from the many different ways in which MR signal may be produced and processed, offering a variety of contrast mechanisms and flexible slice positioning. For example, pulse sequence parameters can be changed dynamically during real-time imaging [Hardy et al. 1993; Holsinger et al. 1990; Kerr et al. 1997] to alter the imaging slice position or contrast as needed for different stages of an examination or invasive procedure [Lederman et al. 2002]. These capabilities have been used for delivery and immediate visualization of intra-myocardial injections of stem cells mixed with a contrast agent [Dick et al. 2003; Kraitchman et al. 2003], and for renal artery stenting [Elgort et al. 2006], among others [Henk et al. 2005; Lederman 2005]. Multiple parallel or oblique slices may be imaged in rapid succession to provide more complete views of a tortuous blood vessel or other anatomical structures such as heart valves, and these slices can be displayed together in a three-dimensional (3D) rendering [Guttman et al. 2002; Lorenz et al. 2005; Quick et al. 2003]. Receiver coils embedded in interventional and surgical devices can be used for device tracking [Feng et al. 2005; McVeigh et al. 2006; Zuehlsdorff et al. 2004], near-field imaging [Atalar et al. 1998; Hillenbrand et al. 2004], or the coil locations may be visualized by colorizing images reconstructed from device coil signals and blending them with grayscale images produced from surface coil signals [Aksit et al. 2002; Guttman et al. 2002; Quick et al. 2003; Serfaty et al. 2000]. The color-highlighted images indicate the positions of invasive devices with anatomical context.

Many of the techniques used for intravascular interventions can be applied directly to the guidance of minimally invasive surgical procedures. For some surgical procedures such as heart valve replacement and repair, percutaneous intravascular methods [Babaliaros et al. 2006; Kuehne et al. 2004] as well as minimally invasive surgical approaches [Horvath et al. 2007] are under active investigation. These techniques present different balances between risk and benefit. The open-chest surgical approach is associated with higher morbidity, but direct access allows superior visualization of anatomy and manipulation of devices for a more durable therapy. The percutaneous methods reduce trauma, but therapeutic devices must be designed for catheter delivery through blood vessels, a constraint which may compromise the performance and durability of the device and therapy. In

addition, some patients with stenotic cardiovascular disease may not be candidates for the percutaneous intervention. With a minimally invasive surgical approach, it may be possible to achieve the best of both surgical and percutaneous techniques reducing trauma while providing durable therapy. This goal is feasible using rtMRI to guide the procedure and monitor the progress of therapy.

14.2 Interventional MR Imaging System

14.2.1 Magnet Configuration

Older generations of MR imaging systems used magnets either of the so-called, closed “doughnut” configuration, with a bore too deep and narrow to allow adequate access to the surgical site, or the open “double pancake” configuration, which allowed superior access but at reduced gradient performance and image quality/speed. These systems have been used in MR-guided therapeutic interventions with success [Blanco et al. 2005; Schulz et al. 2004], but with imaging performance below that which is obtainable on a scanner designed for cardiac applications.

Newer technologies have yielded an effective compromise. Closed bore designs with shorter depth and wider opening, such as the 1.5 T Magnetom Espree (Siemens Medical Solutions Diagnostics, Tarrytown, N.Y. and Los Angeles, CA) with a bore opening 120 cm long by 70 cm wide, are providing greater accessibility with imaging performance rivaling that of many cardiac scanners. Imaging field-of-view (FOV) is reduced to 30 cm, but this has been demonstrated to be adequate for many cardiac interventions. This magnet bore is sufficiently short for a surgeon to reach the center of the magnet, and wide enough to allow placement and manipulation of instruments over the patient’s body. With the heart positioned at the center of the magnet, the short bore also allows better access to the head by anesthesiologists and nurses.

14.2.2 Interventional Imaging Platform

The platform that we have developed at the National Heart, Lung, and Blood Institute (NHLBI) at the National Institutes of Health (NIH) for interventional rtMRI utilizes clinical MR 1.5 T scanners (Sonata with eight receiver channels, Espree with 12 channels, and Avanto with 32 channels, Siemens Medical Solutions Diagnostics), with additional software for sockets communication over Gigabit Ethernet with a Linux workstation (8-CPU, 64-bit, AMD Opteron, HPC Systems, San Jose, CA) running custom software for rapid image reconstruction, display, and 3D rendering [Guttman et al. 2002, 2003a]. The workstation is connected directly to the image reconstruction computer of the MR scanner for quick access to the raw echo data. The reconstruction and display software takes advantage of parallel

processing by farming out tasks to different computing threads, which can run concurrently on different CPUs. Threads are created for individual processing of data from each receiver channel, combination of the data, graphical display, communications, and other tasks that can be executed in parallel. Open source packages and standards are used wherever possible: Fast Fourier transforms are performed using the FFTW library (fftw.org), graphics and user interface are implemented using OpenGL and GLUT (opengl.org).

At the beginning of a scan, imaging parameters are sent from the scanner to the workstation for initialization of the reconstruction program. At the end of each image acquisition, a packet of data containing dynamic imaging parameters and the raw MR data is sent to the workstation. Commands are sent to the scanner in response to user input via the same network interface.

14.2.3 Pulse Sequences and Image Reconstruction

MR data is acquired in the frequency domain (k -space) and reconstructed into an image by Fourier transformation. Real-time MR imaging requires an efficient pulse sequence, i.e., one that covers k -space in a short time. This is often accomplished by acquiring many data points in each repetition, such as in echo-planar or spiral, or by using sequences with inherently short repetition times (TR), such as gradient-recalled echo or steady-state free precession (SSFP, a.k.a. True FISP, b-FFE, FIESTA) [Oppelt et al. 1986]. The NHLBI implementation uses SSFP for rapid, high signal-to-noise ratio (SNR) consecutive imaging of multiple slices. Imaging parameters are tailored to the procedure: although high frame rates are available, spatial resolution and image quality are given priority over imaging speed, thus reported frame rates are well below the maximum attainable. The imaging frame rate is then increased using variable rate view sharing or TSENSE [Guttman et al. 2003a; Kellman et al. 2001]. Both of these methods accelerate image acquisition by skipping phase encoding lines. For example, at acceleration rate 2, odd and even lines are acquired in alternating acquisitions. For acceleration rate N , every N th line is acquired, incrementing the starting line for each image acquisition. This causes ghosting artifacts of moving objects, which are suppressed by TSENSE using dynamic estimates of the coil sensitivities.

TSENSE is one of the several parallel imaging techniques such as SMASH [Sodickson and Manning 1997], SENSE [Pruessmann et al. 1999], and GRAPPA [Griswold et al. 2002], which accelerate imaging by undersampling k -space, and use the local sensitivity map of each coil element to either fill in the gaps in k -space or remove undersampling artifacts in image space. Modern scanners feature up to 32 channels, which provide enough independent information for parallel imaging methods to achieve an acceleration factor of four with good image quality. Other acceleration methods do

not require multiple coils and use the fact that the samples in a typical time series of image data are correlated in time (UNFOLD [Madore et al. 1999], or both k -space and time (k - t BLAST [Tsao et al. 2003]).

Since SSFP is a steady-state imaging sequence, care must be taken when disrupting the steady state for multiple slice imaging or image preparation such as fat suppression. In the NHLBI implementation for these cases, the magnetization is stored longitudinally (along the z -axis) after each image acquisition, using a “closing” sequence ($-\alpha/2$; gradient spoil) [Scheffler et al. 2001], followed by the preparation and an “opening” sequence (gradient spoil; $\alpha/2$; $-\alpha$; dummy pulses) on the new slice. Fat-selective saturation is achieved by either a typical fat selective RF pulse or one of the quicker off-resonance saturation schemes as described elsewhere [Derbyshire et al. 2005; Santos et al. 2003].

14.2.4 Interactive Imaging Features

Graphical user interfaces for rtMRI guidance of interventional procedures have been under active development. The first systems allowed basic real-time imaging with a single adjustable imaging plane [Holsinger et al. 1990; Morton et al. 1997]. Subsequent systems added many of the features described above [Aksit et al. 2002; Guttman et al. 2002; Nayak et al. 2001; Quick et al. 2003]. Automatic image parameter adjustment in response to motion of a device being tracked has also been investigated [Elgort et al. 2003; Zuehlsdorff et al. 2004].

Recent work has shown the utility of device-only projection imaging, an interactive imaging mode where slice-selection is turned off and images are produced using signal from only the invasive devices [Peters et al. 2003], for views that resemble X-ray fluoroscopy. The entire active portion of the device is displayed against a dark background. This mode can be switched on and off during scanning for any slice to give a quick glance at an active device that may have escaped the thin-slice imaging plane.

Derived from this technique is adaptively oriented projection navigation (PRONAV), which is designed to facilitate steering of an active device towards target tissue. A device-only projection image and at least one standard thin-slice image are displayed together in a 3D rendering, all updated using real-time imaging. As the user interactively rotates the 3D rendering, the scanner automatically changes the projection direction, analogous to changing X-ray gantry position during fluoroscopy. This provides a real-time 3D view of the catheter position and trajectory with respect to the thin-slice image plane. For anatomical context, the thin-slice image is positioned to contain target tissue, and the combination of projection and thin-slice views can be used to navigate the device towards the target.

The NHLBI rtMRI implementation contains the projection imaging features and many other interactive features, which can be controlled by simple keyboard or mouse operation without stopping the scanner. Below is an abbreviated list of interactive features available [Guttman et al. 2002, 2003a; Raman et al. 2005]:

1. Display each slice in separate windows, as well as a 3D rendering where they are shown at their respective locations in space (see Fig. 14.1 and Fig. 14.2). This provided simultaneous views of all slices and devices in one window from any angle.

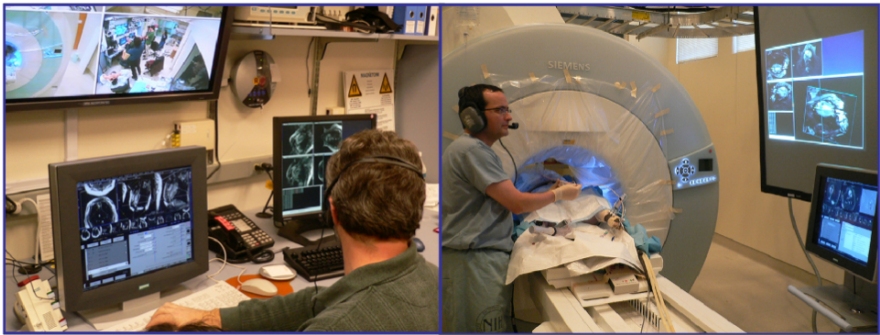


Fig. 14.1. The console room (*left*) and inside magnet room (*right*) during a swine experiment. Output from the custom reconstruction engine is rear projected onto the magnet room screen. The MRI scanner console is displayed on a remote monitor (*right*). MRI scanner console. Headsets are used for communication during scans

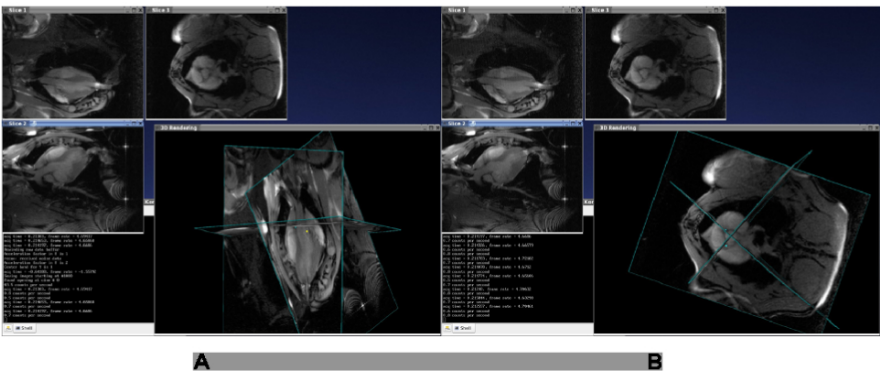


Fig. 14.2. Real-time multislice imaging before placement of a bioprosthetic aortic valve in swine. Three 2D slices are shown both individually and in a 3D rendering at their respective positions. On the live display, colored dots mark the positions of LAD and RCA ostia and the level of the aortic valve annulus. Two viewing angles of the 3D rendering are displayed A and B, showing long and short axis views of the multiple slice scan, respectively. A Video (Movie 14.1) demonstrating the dynamic interaction depicted by this figure is included with the DVD accompanying this book

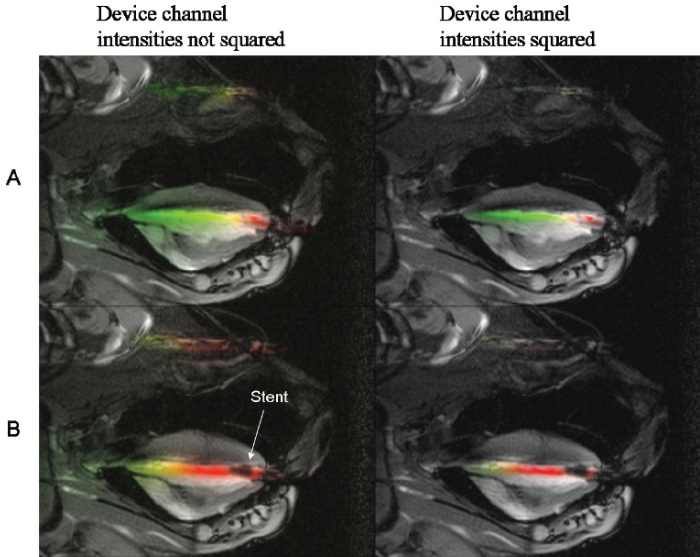


Fig. 14.3. (A) The central guide wire (*green*) is advanced through the LV and aortic valve. (B) The catheter with the stent/valve (*dark region* on the catheter) and second guide wire attached to the side of the stent (*red*) is advanced along the central lumen guide wire. The right column shows how squaring the intensity of the device images sharpens the appearance of the devices in the images and reduces the background noise from the device channels

2. Change the slice position/orientation using the standard scanner slice prescription interface.
3. Enable/disable acquisition of selected slices. This was often used when slices were initially prescribed for all stages of the procedure, and then only those needed at the time were enabled.
4. Highlight device channels in different colors, blended with grayscale images from surface coils (see Fig. 14.2). The device signal magnitude can be squared to sharpen the device profile.
5. Marking of reference points. Reference points are displayed in the 3D rendering and persist until deleted. This was used to mark anatomical features for device positioning (see Fig. 14.2).
6. Enable/disable squaring of device channel intensity. Squaring sharpens the device profile for more accurate localization.
7. Enable/disable device-only projection view on selected slices to show entire device if it exited from the thin slice.
8. Enable/disable adaptive projection navigation (PRONAV) mode for 3D projection views of the device.
9. Use non-selective saturation to darken background and isolate T1-shortening contrast agent (see Fig. 14.3).

10. Change acceleration factor.
11. Enable subtraction imaging for enhancing contrast injections.
12. Enable saving of raw data to files. The same program can be used at a later time to review the images with the same or different options for reconstruction or display. Several display and rendering parameters (such as 3D rendering orientation, highlight colors, window positions) are also saved. Post-procedure review therefore can mimic how the images were displayed during the actual procedure.

14.2.5 Invasive Devices and Experiments

Several custom-made active interventional devices, such as guide wires and catheters incorporating an active solenoid coil at the distal tip or loopless antenna [Ocali and Atalar 1997], were employed for in vivo experiments to develop the features described above.

One such device is a dual-channel injection catheter designed by S. Smith and G. Scott [Dick et al. 2003], based on the X-ray compatible Stiletto catheter (Boston Scientific, Inc.), which had an antenna along its shaft and a small coil near the tip. Experiments were performed on swine with previously induced infarcts, as described by Dick et al. [2003]. Two imaging planes were prescribed for real-time imaging: (1) Long-axis “candy cane” view showing ascending and descending aorta, aortic valve, and left ventricle (LV); (2) LV short-axis plane containing infarcted tissue, seen by delayed hyper-enhancement after contrast injection. The catheter was steered into the LV using the candy cane view. Then the short-axis view was turned on and PRONAV enabled on the candy cane view to guide navigation of the catheter towards the border regions of the infarcts.

Another device is an active loopless antenna guide-wire with a flexible tip [Raval et al. 2006b]. Two of these devices were used to guide minimally invasive surgical implantation of bioprosthetic aortic valves. One active guide-wire was used to cross the native aortic valve antegrade via a left ventricular transapical approach. The valve was affixed to a platinum stent and compressed onto the outer balloon of a BiB catheter. The second guide-wire was loosely sutured to the outside of the stent, along one of the commissures of the valve. Three oblique slices were prescribed: (1) axial view of the aortic valve; (2) long axis image containing the LAD ostium, aortic valve, and trocar; and (3) long axis image containing the RCA ostium, aortic valve, and trocar. The axial image was interactively translated above the valve to show the ostia of the LAD and RCA, which were then marked for reference. The aortic valve annulus position was similarly marked on one of the long-axis images. Multiple-slice imaging with color-highlighted active guide-wires and anatomical reference markers were then used to guide the delivery trajectory and positioning of the stent/valve.

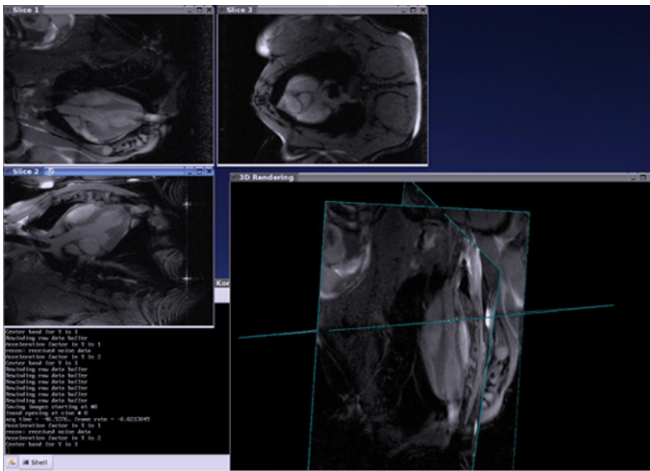
Typical imaging parameters for cardiac interventional experiments were as follows: matrix size of 108×192 ; TR/TE = 3.84/1.92 ms; bandwidth,

1,000 Hz/pixel or higher; excitation RF pulse $\alpha = 45^\circ$; $3/4$ partial phase-encode acquisition with homodyne detection for k -space filling [Noll et al. 1991]; and acceleration rate of 2. For higher quality imaging of more stationary tissues such as peripheral vessels, the parameters were typically changed to 168×224 matrix, 800 Hz/pixel bandwidth, full phase-encode acquisition, and acceleration rate of 2 or 3. Frame rate ranged from 3 to 8 per second, depending on the choice of imaging parameters.

The Siemens torso phased-array coil or a custom design surface coil (Nova Medical, Wilmington, MA) was placed on the ventral surface. Spine coils were turned on only when necessary, e.g., for imaging the aorta or some peripheral vessels, otherwise they were turned off to allow smaller FOV and increased spatial resolution. One or two receiver channels were used for device-mounted coils. The scanner was set up to function normally while MR echo data were simultaneously transferred to the workstation for custom reconstruction and display. Image reconstruction on the scanner can be turned off in case a high data rate (e.g., from using many receiver channels) causes it to lag behind data acquisition.

14.2.6 Room Setup

Figure 14.1 shows the console room (left) and magnet room (right), representative of our typical configuration during interventional experiments on animal models. Several displays are used in both rooms to monitor



Movie 14.1. (This movie can be found on the DVD accompanying this book). Real-time multislice imaging before placement of a bioprosthetic aortic valve in swine. Three 2D slices are shown individually and in a 3D rendering at their respective positions. *Cyan dots* mark the positions of LAD and RCA ostia; the *yellow dot* marks the level of the aortic valve annulus. The 3D rendering is rotated to view the slices from different angles, for better understanding of the slice positions in anatomical context.

the function of the scanner, external workstation, and physiology [Guttman et al. 2003b]. Team members wear custom-designed communication headsets (Magnacoustics, Atlantic Beach, NY) with noise-canceling optical microphones (Phone-Or, Or-Yehuda, Israel) to talk to each other during scanning for imaging parameter changes, timing during injections, or saving data. Slice position and orientation changes were performed interactively in the graphical prescription interface on the scanner console. Complex scanner controls dictate that someone other than the surgeon will adjust imaging parameters, and thus good voice communication between the physician and operator is essential.

14.3 Initial Preclinical Procedures

Some of the important features of the system are illustrated in Fig. 14.2. This figure shows a screen capture on the external workstation before placement of a bioprosthetic aortic valve in swine. Multiple oblique slices were acquired in succession and displayed at their respective locations on the 3D rendering. Heart function can be monitored in either long-axis view if a single slice is enabled. The trocar is seen in the long-axis images, having been inserted through the LV apex. The coronary ostia and aortic valve annulus were visible in the real-time images. For anatomical reference, their positions were marked in the 2D images and were displayed in the 3D rendering (ostia and annulus in cyan and yellow dots, respectively). Two viewing angles of the 3D rendering are displayed (Fig. 14.2a,b), showing long and short axis views of the multiple slice scan, respectively. There is a movie (Movie 14.1) on the CD included with this book, which shows this with interactive rotations of the 3D rendering are shown in Movie 14.1, which is on the DVD included with this book.

Figure 14.3 shows images where signal from the active guide-wires was reconstructed separately from that of the surface coils, color highlighted, and blended. The central active guide-wire was clearly seen (green) as it was steered through the aortic valve (Fig. 14.3a). The second active guide-wire affixed to the side of the stent (red) as well as the stent itself (darkened region from RF shielding) were easily seen as the device was advanced through the LV (Fig. 14.3b). Note that the red and green colors blend to yellow in regions where both active guide wires are visible. The right column shows how squaring the intensity of the device images sharpens the appearance of the devices in the images and reduces the background noise from the device channels.

The axial image in Fig. 14.4 provided feedback when rotating the valve to position a commissure between the coronary ostia (cyan dots) before deployment. The active guide wire affixed to the side of the stent (green) indicated the commissure position. In Fig. 14.5, the proximal edge

of the stent/valve was lined up with the annulus marker (yellow dot, c). This integrated information facilitated placement of the stent/valve at the correct location using real-time MRI guidance.

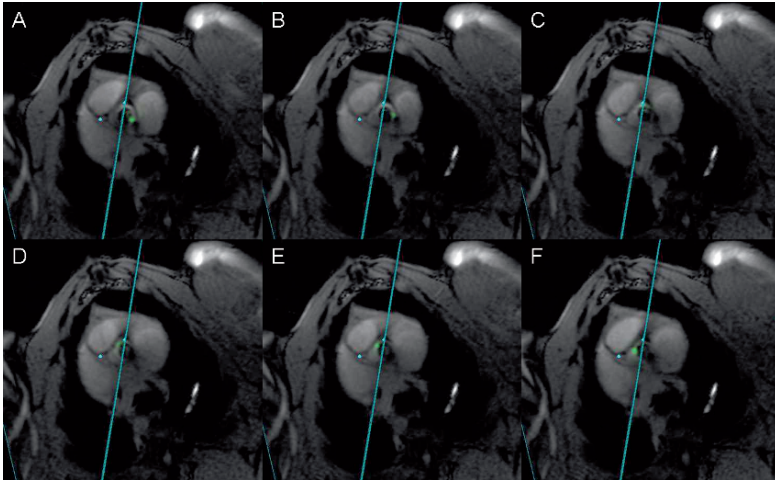


Fig. 14.4. The stent/valve is rotated using rtMRI feedback. The guide wire affixed to the side of the stent (*green*) indicates the position of a commissure. The practitioner rotates the catheter to position the commissure between the coronary ostia

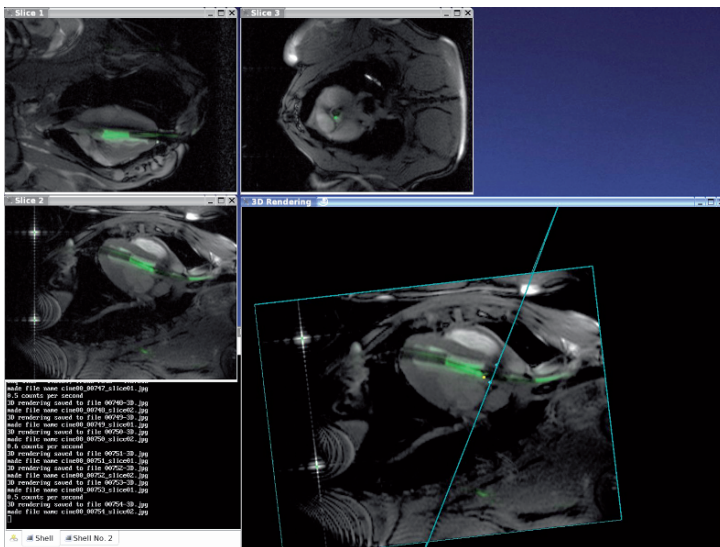


Fig. 14.5. The practitioner advances the stent until the proximal edge lines up with the marker, indicating the aortic valve annulus level (*yellow dot*)

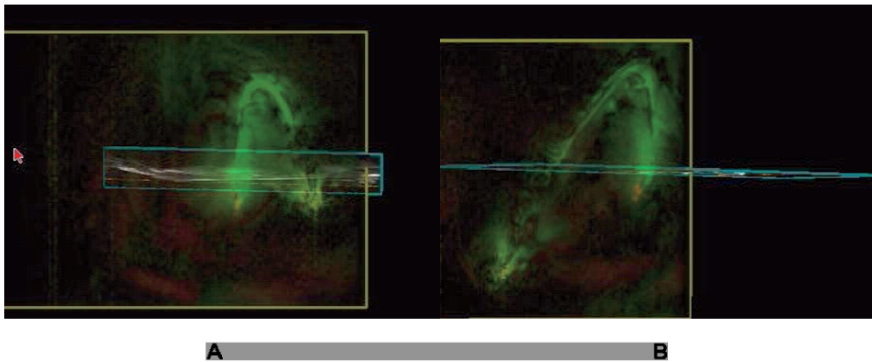
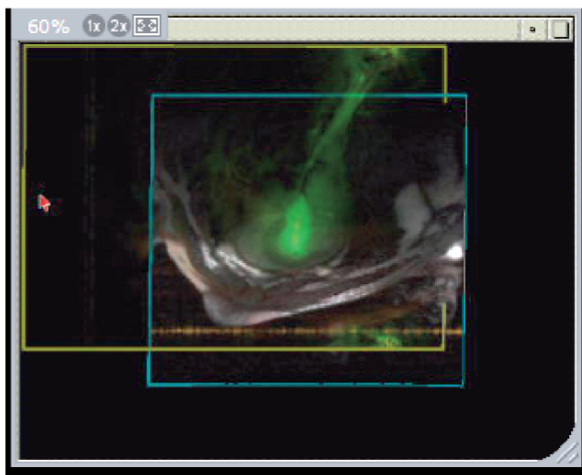


Fig. 14.6. Adaptive projection navigation (PRONAV) is illustrated in this basic example. The projection image is displayed along with a thin slice image **A**. When the 3D rendering is interactively rotated **B**, the projection direction is automatically updated, providing a different view of the device. The device is an injection catheter containing two receivers: a small coil at the tip (*red*) and a loopless antenna along the shaft (*green*)



Movie 14.2. (This movie can be found on the DVD accompanying this book). Adaptive projection navigation (PRONAV) is illustrated in this basic example. At first, an LV short axis image is seen. The full extent of the device is seen when device-only projection imaging is turned on. The 3D rendering is then rotated down then horizontally, revealing the trajectory of the injection catheter. The projection image is displayed along with a thin slice image. When the 3D rendering is interactively rotated, the projection direction is automatically updated, providing a different view of the device. The device is an injection catheter containing two receivers: a small coil at the tip (*red*) and a loopless antenna along the shaft (*green*).

Figure 14.6 and Movie 14.2 (on the included CD) demonstrate the basic function of adaptive projection navigation (PRONAV) in a percutaneous targeting experiment, using an active injection catheter containing two

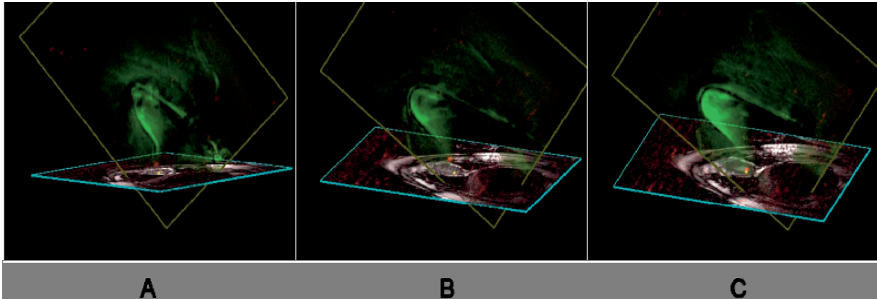
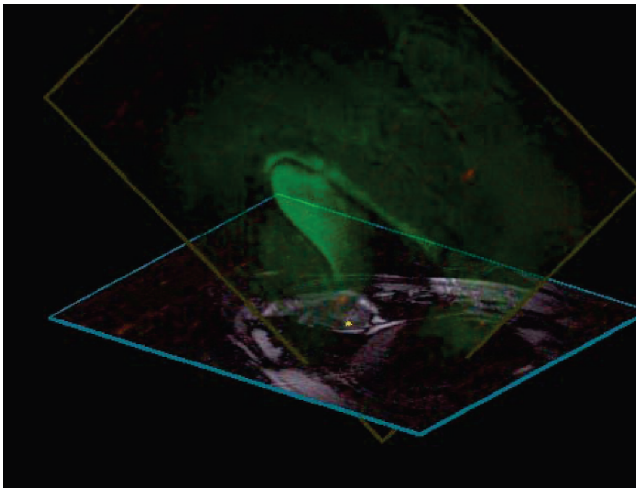


Fig. 14.7. PRONAV is used for real-time 3D visualization of an active catheter and navigation towards infarct border tissue in a 2D image plane. A *yellow dot* marks the target tissue. The device is the same as that in Fig. 14.6. The rendering is manually rotated during the scan to see the device trajectory from different angles, giving a 3D effect. Knowledge of the device trajectory is used to advance the tip of the device toward the target tissue



Movie 14.3. (This movie can be found on the DVD accompanying this book). PRONAV imaging is used in an intra-myocardial injection experiment. This 3D rendering shows a thin-slice image, a device-only projection image, and a yellow marker indicating a target on the endocardium. As the user rotates the rendering, the projection direction is continually oriented normal to the viewing screen. This allows appreciation of the full trajectory of the device from any angle, imparting a 3D viewing effect. Updating of the thin-slice image stops while rotating the rendering for better interactivity with the projection image. Knowledge of the device trajectory is used to advance the tip of the device toward the target tissue.

receivers: a small coil at the tip (red) and a loopless antenna along the shaft (green). The projection image of the device only is displayed together with a thin slice image (a). When the 3D rendering is interactively rotated (b), the projection direction is automatically updated, providing a different view of the device. The interactive technique gives a 3D perception of device trajectory, better appreciated in moving rather than static pictures. In Fig. 14.7 and Movie 14.3 (on the included CD), PRONAV is used for navigation towards infarct border tissue in a 2D image plane [Dick et al. 2003].

Projection imaging allowed continuous visualization of the device in 3D when the rendering was rotated. Targeting of infarct borders was enhanced, since regions of reduced cardiac function and delayed hyper-enhancement (post-contrast) were observable in the thin-slice image. This interactive technique gave 3D feedback about device trajectory with respect to the imaging slice and simplified catheter steering toward target tissue in the imaging plane.

14.4 Discussion

An interactive real-time MR imaging environment initially developed for use in intravascular procedures [Guttman et al. 2003b] has been adapted to guide minimally invasive cardiovascular surgical procedures such as aortic valve placement. Many features were implemented that exploit the advantages of MRI: enhancing visualization of separate antennae or coils mounted on invasive devices, providing multiple oblique slices that are easily adjusted, rendering all slices and landmarks in 3D, accelerated imaging and projection imaging modes to see the entire trajectory of a device receiving signal along its shaft.

The system has been used by our group in a number of preclinical studies in swine, including intra-myocardial injection of stem cells [Dick et al. 2003], endovascular repair of abdominal aortic aneurysms [Raman et al. 2005], stenting of aortic coarctation [Raval et al. 2005], recanalization of chronic total occlusions [Raval et al. 2006b], atrial-septal puncture and balloon septostomy [Raval et al. 2006a], and catheterization in humans [Dick et al. 2005]. In this chapter, we have shown results from feasibility experiments in which the system was used to guide minimally invasive aortic valve replacement. Separate experiments were previously performed to improve catheter navigation for intra-myocardial injection, all using rtMRI for visual feedback while manipulating invasive devices. The particular needs of these applications have driven the development of the system over the last several years.

Real-time imaging of multiple oblique slices offers many potential advantages. Different views of complicated anatomy may be simultaneously displayed and individual slices can be interactively turned on or off during a scan as needed. Another important use would be to provide continuous monitoring of function (e.g., heart motion) in one view during an intervention requiring a different view. Also of benefit would be to allow a

different sequence or parameters to be run for different slices. This would increase the range of information provided by the real-time imaging.

High performance hardware was used to minimize image reconstruction latency. As reported, typical frame rates ranged from 3 to 8 per second, depending on choice of parameters. Much higher frame rates, in excess of 30 per second, were sustainable by the system when using small k -space matrix (such as 64×128), view sharing, and eight receiver channels. This small matrix does not result in adequate image quality, but was useful to gauge the limits of the reconstruction and display pipeline. As of this writing, better raw data throughput and a faster reconstruction computer are required to handle real-time processing of 32-channel data with high acceleration rates and larger matrix.

The minimally invasive valve replacement experiment was performed on a Siemens 1.5 T Espree scanner. This magnet features a bore with wider diameter (70 cm) and shorter length (120 cm) than has been common until now, which provided easier access to the worksite than the typical 1.5 T magnet bore. One compromise is a smaller imaging volume, which is especially evident using a refocused sequence such as SSFP. However, our experience is that the imaging volume is adequate to perform this intervention without moving the patient table.

Further advancements will incorporate more advanced real-time volume rendering modes, other interactive control modes such as PRONAV, and closed-loop techniques for automatically changing image parameters [Elgort et al. 2006]. An imaging suite such as this can be of benefit to a variety of interventional procedures using real-time MRI guidance.

MRI offers the advantage that the surgeon can see “through” the blood, and morphological landmarks for positioning the device are visible. New short magnet design makes it possible to have high performance real-time MRI available while manipulating the prosthetic valve under image guidance. These advantages render real-time MRI an attractive method to guide interventional procedures. In addition to the aortic valve procedure discussed here, additional target applications are mitral, pulmonary, and tricuspid valve replacements or repairs [Boudjemline et al. 2004, 2005; Buchbinder and Cosgrove 1998; Mihaljevic et al. 2004].

Acknowledgment

The authors thank Joni Taylor, Kathy Lucas, Shawn Kozlov, and Timothy Hunt for animal care and support. Much of the development of rtMRI interventional procedures was a collaboration with the following investigators: Cenghizhan Ozturk, MD, PhD; Parag V. Karmarkar, MS; Amish N. Raval, MD; Venkatesh K. Raman, MD; Alexander J. Dick, MD; Ranil DeSilva, MBBS, PhD; Ming Li, PhD. This work was supported through the Intramural Research Program of the National Heart Lung and Blood Institute, NIH, DHHS.

References

- Aksit P, Derbyshire JA, Serfaty JM, and Atalar E. (2002). Multiple field of view MR fluoroscopy. *Magn Reson Med*, 47(1), 53–60
- Atalar E, Kraitchman DL, Carkhuff B, Lesho J, Ocali O, Solaiyappan M, Guttman MA, and Charles HK, Jr. (1998). Catheter-tracking FOV MR fluoroscopy. *Magn Reson Med*, 40(6), 865–872
- Babaliaros V, Cribier A, and Agatiello C. (2006). Surgery insight: Current advances in percutaneous heart valve replacement and repair. *Nat Clin Pract Cardiovasc Med*, 3(5), 256–264
- Blanco RT, Ojala R, Kariniemi J, Perala J, Niinimaki J, and Tervonen O. (2005). Interventional and intraoperative MRI at low field scanner – A review. *Eur J Radiol*, 56(2), 130–142
- Boudjemline Y, Agnoletti G, Bonnet D, Sidi D, and Bonhoeffer P. (2004). Percutaneous pulmonary valve replacement in a large right ventricular outflow tract: An experimental study. *J Am Coll Cardiol*, 43(6), 1082–1087
- Boudjemline Y, Pineau E, Borenstein N, Behr L, and Bonhoeffer P. (2005). New insights in minimally invasive valve replacement: Description of a cooperative approach for the off-pump replacement of mitral valves. *Eur Heart J*, 26(19), 2013–2017
- Buchbinder BR and Cosgrove GR. (1998). Cortical activation MR studies in brain disorders. *Magn Reson Imaging Clin N Am*, 6(1), 67–93
- Derbyshire JA, Herzka DA, and McVeigh ER. (2005). S5FP: Spectrally selective suppression with steady state free precession. *Magn Reson Med*, 54(4), 918–928
- Dick AJ, Guttman MA, Raman VK, Peters DC, Pessanha BS, Hill JM, Smith S, Scott G, McVeigh ER, and Lederman RJ. (2003). Magnetic resonance fluoroscopy allows targeted delivery of mesenchymal stem cells to infarct borders in Swine. *Circulation*, 108(23), 2899–2904
- Dick AJ, Raman VK, Raval AN, Guttman MA, Thompson RB, Ozturk C, Peters DC, Stine AM, Wright VJ, Schenke WH, and Lederman RJ. (2005). Invasive human magnetic resonance imaging: Feasibility during revascularization in a combined XMR suite. *Catheter Cardiovasc Interv*, 64(3), 265–274
- Doty DB, Flores JH, and Doty JR. (2000). Cardiac valve operations using a partial sternotomy (lower half) technique. *J Card Surg*, 15(1), 35–42
- Elgort DR, Hillenbrand CM, Zhang S, Wong EY, Rafie S, Lewin JS, and Duerk JL. (2006). Image-guided and -monitored renal artery stenting using only MRI. *J Magn Reson Imaging*, 23(5), 619–627
- Elgort DR, Wong EY, Hillenbrand CM, Wacker FK, Lewin JS, and Duerk JL. (2003). Real-time catheter tracking and adaptive imaging. *J Magn Reson Imaging*, 18(5), 621–626
- Feng L, Dumoulin CL, Dashnaw S, Darrow RD, Guhde R, Delapaz RL, Bishop PL, and Pile-Spellman J. (2005). Transfemoral catheterization of carotid arteries with real-time MR imaging guidance in pigs. *Radiology*, 234(2), 551–557
- Griswold MA, Jakob PM, Heidemann RM, Nittka M, Jellus V, Wang J, Kiefer B, and Haase A. (2002). Generalized autocalibrating partially parallel acquisitions (GRAPPA). *Magn Reson Med*, 47(6), 1202–1210

- Guttman MA, Kellman P, Dick AJ, Lederman RJ, and McVeigh ER. (2003a). Real-time accelerated interactive MRI with adaptive TSENSE and UNFOLD. *Magn Reson Med*, 50(2), 315–321
- Guttman MA, Lederman RJ, and McVeigh ER. (2003b). The cardiovascular interventional MRI suite: Design considerations. in *Cardiovascular Magnetic Resonance: Established and Emerging Applications*, ed. by Lardo A, Fayad ZA, Fuster V, and Chronos N, (Martin Dunitz, London)
- Guttman MA, Lederman RJ, Sorger JM, and McVeigh ER. (2002). Real-time volume rendered MRI for interventional guidance. *J Cardiovasc Magn Reson*, 4(4), 431–442
- Hardy CJ, Darrow RD, Nieters EJ, Roemer PB, Watkins RD, Adams WJ, Hattes NR, and Maier JK. (1993). Real-time acquisition, display, and interactive graphic control of NMR cardiac profiles and images. *Magn Reson Med*, 29(5), 667–673
- Henk CB, Higgins CB, and Saeed M. (2005). Endovascular interventional MRI. *J Magn Reson Imaging*, 22(4), 451–460
- Hillenbrand CM, Elgort DR, Wong EY, Reykowski A, Wacker FK, Lewin JS, and Duerk JL. (2004). Active device tracking and high-resolution intravascular MRI using a novel catheter-based, opposed-solenoid phased array coil. *Magn Reson Med*, 51(4), 668–675
- Holsinger AE, Wright RC, Riederer SJ, Farzaneh F, Grimm RC, and Maier JK. (1990). Real-time interactive magnetic resonance imaging. *Magn Reson Med*, 14(3), 547–553
- Horvath KA, Guttman M, Li M, Lederman RJ, Mazilu D, Kocaturk O, Karmarkar PV, Parag V, Hunt T, Kozlov S, and McVeigh ER. (2007). Beating heart aortic valve replacement using real-time MRI guidance. *Innovations: Technology and Techniques in Cardiothoracic and Vascular Surgery*. 2(2): 51–55
- Kellman P, Epstein FH, and McVeigh ER. (2001). Adaptive sensitivity encoding incorporating temporal filtering (TSENSE). *Magn Reson Med*, 45(5), 846–852
- Kerr AB, Pauly JM, Hu BS, Li KC, Hardy CJ, Meyer CH, Macovski A, and Nishimura DG. (1997). Real-time interactive MRI on a conventional scanner. *Magn Reson Med*, 38(3), 355–367
- Kraitchman DL, Heldman AW, Atalar E, Amado LC, Martin BJ, Pittenger MF, Hare JM, and Bulte JW. (2003). *In vivo* magnetic resonance imaging of mesenchymal stem cells in myocardial infarction. *Circulation*, 107(18), 2290–2293
- Kuehne T, Yilmaz S, Meinus C, Moore P, Saeed M, Weber O, Higgins CB, Blank T, Elsaesser E, Schnackenburg B, Ewert P, Lange PE, and Nagel E. (2004). Magnetic resonance imaging-guided transcatheter implantation of a prosthetic valve in aortic valve position: Feasibility study in swine. *J Am Coll Cardiol*, 44(11), 2247–2249
- Lederman RJ. (2005). Cardiovascular interventional magnetic resonance imaging. *Circulation*, 112(19), 3009–3017
- Lederman RJ, Guttman MA, Peters DC, Thompson RB, Sorger JM, Dick AJ, Raman VK, and McVeigh ER. (2002). Catheter-based endomyocardial injection with real-time magnetic resonance imaging. *Circulation*, 105(11), 1282–1284
- Lorenz CH, Kirchberg KJ, Zuehlsdorff S, Speier P, Caylus M, Borys W, Moeller T, and Guttman MA. (2005). Interactive Frontend (IFE): A Platform for Graphical MR Scanner Control and Scan Automation. *ISMRM*, Miami, 7–13 May

- Lutter G, Ardehali R, Cremer J, and Bonhoeffer P. (2004). Percutaneous valve replacement: Current state and future prospects. *Ann Thorac Surg*, 78(6), 2199–2206
- Madore B, Glover GH, and Pelc NJ. (1999). Unaliasing by fourier-encoding the overlaps using the temporal dimension (UNFOLD), applied to cardiac imaging and fMRI. *Magn Reson Med*, 42(5), 813–828
- McVeigh ER, Guttman MA, Lederman RJ, Li M, Kocaturk O, Hunt T, Kozlov S, and Horvath KA. (2006). Real-time interactive MRI guided cardiac surgery: aortic valve replacement using a direct apical approach. *Magn Reson Med*, 56(5), 958–964
- Mihaljevic T, Cohn LH, Unic D, Aranki SF, Couper GS, and Byrne JG. (2004). One thousand minimally invasive valve operations: Early and late results. *Ann Surg*, 240(3), 529–534
- Morton RE, Bonas R, Minford J, Kerr A, and Ellis RE. (1997). Feeding ability in Rett syndrome. *Dev Med Child Neurol*. 39(5), 331–335
- Nayak KS, Pauly JM, Nishimura DG, and Hu BS. (2001). Rapid ventricular assessment using real-time interactive multislice MRI. *Magn Reson Med*, 45(3), 371–375
- Noll DC, Nishimura DG, and Macovski A. (1991). Homodyne detection in magnetic resonance imaging. *IEEE Trans Med Imag*, 10(2), 154–163
- Ocali O and Atalar E. (1997). Intravascular magnetic resonance imaging using a loopless catheter antenna. *Magn Reson Med*, 37(1), 112–118
- Oppelt A, Graumann R, Barfuß H, Fischer H, Hartl W, and Scajor W. (1986). FISP – A new fast MRI sequence. *Electromedica*, 54(1), 15–18
- Peters DC, Lederman RJ, Dick AJ, Raman VK, Guttman MA, Derbyshire JA, and McVeigh ER. (2003). Undersampled projection reconstruction for active catheter imaging with adaptable temporal resolution and catheter-only views. *Magn Reson Med*, 49(2), 216–222
- Pruessmann KP, Weiger M, Scheidegger MB, and Boesiger P. (1999). SENSE: sensitivity encoding for fast MRI. *Magn Reson Med*, 42(5), 952–962
- Quick HH, Kuehl H, Kaiser G, Hornscheidt D, Mikolajczyk KP, Aker S, Debatin JF, and Ladd ME. (2003). Interventional MRA using actively visualized catheters, TrueFISP, and real-time image fusion. *Magn Reson Med*, 49(1), 129–137
- Raman VK, Karmarkar PV, Guttman MA, Dick AJ, Peters DC, Ozturk C, Pessanha BS, Thompson RB, Raval AN, DeSilva R, Aviles RJ, Atalar E, McVeigh ER, and Lederman RJ. (2005). Real-time magnetic resonance-guided endovascular repair of experimental abdominal aortic aneurysm in swine. *J Am Coll Cardiol*, 45(12), 2069–2077
- Raval AN, Karmarkar PV, Guttman MA, Ozturk C, Desilva R, Aviles RJ, Wright VJ, Schenke WH, Atalar E, McVeigh ER, and Lederman RJ. (2006a). Real-time MRI guided atrial septal puncture and balloon septostomy in swine. *Catheter Cardiovasc Interv*, 67(4), 637–643
- Raval AN, Karmarkar PV, Guttman MA, Ozturk C, Sampath S, DeSilva R, Aviles RJ, Xu M, Wright VJ, Schenke WH, Kocaturk O, Dick AJ, Raman VK, Atalar E, McVeigh ER, and Lederman RJ. (2006b). Real-time magnetic resonance imaging-guided endovascular recanalization of chronic total arterial occlusion in a swine model. *Circulation*, 113(8), 1101–1107

- Raval AN, Telep JD, Guttman MA, Ozturk C, Jones M, Thompson RB, Wright VJ, Schenke WH, DeSilva R, Aviles RJ, Raman VK, Slack MC, and Lederman RJ. (2005). Real-time magnetic resonance imaging-guided stenting of aortic coarctation with commercially available catheter devices in Swine. *Circulation*, 112(5), 699–706
- Santos JM, Hargreaves BA, Nayak KS, and Pauly JM. (2003). Real-Time Fat Suppressed SSFP *Proc 11th ISMRM*, Toronto, p. 982
- Scheffler K, Heid O, and Hennig J. (2001). Magnetization preparation during the steady state: Fat-saturated 3D TrueFISP. *Magn Reson Med*, 45(6), 1075–1080
- Schulz T, Puccini S, Schneider JP, and Kahn T. (2004). Interventional and intraoperative MR: Review and update of techniques and clinical experience. *Eur Radiol*, 14(12), 2212–2227
- Serfaty JM, Yang X, Aksit P, Quick HH, Solaiyappan M, and Atalar E. (2000). Toward MRI-guided coronary catheterization: visualization of guiding catheters, guidewires, and anatomy in real time. *J Magn Reson Imaging*, 12(4), 590–594
- Sodickson DK and Manning WJ. (1997). Simultaneous acquisition of spatial harmonics (SMASH): Fast imaging with radiofrequency coil arrays. *Magn Reson Med*, 38(4), 591–603
- Tsao J, Boesiger P, and Pruessmann KP. (2003). *k-t* BLAST and *k-t* SENSE: Dynamic MRI with high frame rate exploiting spatiotemporal correlations. *Magn Reson Med*, 50(5), 1031–1042
- Vassiliades TA, Jr., Block PC, Cohn LH, Adams DH, Borer JS, Feldman T, Holmes DR, Laskey WK, Lytle BW, Mack MJ, and Williams DO. (2005). The clinical development of percutaneous heart valve technology. *J Thorac Cardiovasc Surg*, 129(5), 970–976
- Zuehlsdorff S, Umathum R, Volz S, Hallscheidt P, Fink C, Semmler W, and Bock M. (2004). MR coil design for simultaneous tip tracking and curvature delineation of a catheter. *Magn Reson Med*, 52(1), 214–218